JOURNAL OF GUIDANCE, CONTROL, AND DYNAMICS
Vol. 20, No. 4, July–August 1997

Mass Property Estimation Using Coasting Maneuvers

Sergei Tanygin* and Trevor Williams†
University of Cincinnati, Cincinnati, Ohio 45221-0070

The problem of estimating the mass properties of a spinning rigid body is considered. The parameter estimation method allows determination of both the inertia matrix and the position of the center of mass. The regressor model constructed is nonlinear in measurements but linear in mass properties. It does not involve linearization of the rotational dynamics of a rigid body. Use of coasting maneuvers for inertia estimation is the main feature of the method. This improves inertia estimation, especially in the presence of long coasting phases. A geometrical interpretation of inertia estimation is also introduced. The optimal choice of body-fixed coordinate system and maneuver sequences for mass property estimation are recommended based on stochastic analysis of the method. The method proposed is tested on both simulated and actual on-orbit data.

Nomenclature

$E\{\}$ = expected value
$\bar{\boldsymbol{F}}$ = resultant force vector in body-fixed coordinate system, $[\bar{F}_x \;\; \bar{F}_y \;\; \bar{F}_z]^T$, $\sum_i \boldsymbol{F}_i$
$\boldsymbol{F}_i$ = ith applied force vector
I = inertia matrix relative to center of mass in body-fixed coordinate system
$\hat{\boldsymbol{I}}$ = vector constructed from elements of I, moments and products of inertia, $[I_x \;\; I_y \;\; I_z \;\; -I_{xy} \;\; -I_{xz} \;\; -I_{yz}]^T$
J = quadratic cost function in batch least square estimation
$\boldsymbol{M}$ = total applied torque vector
R = upper triangular matrix in QR decomposition of Φ
$\boldsymbol{R}$ = position vector in body-fixed coordinate system from origin of body-fixed coordinate system to center of mass, $[R_x \;\; R_y \;\; R_z]^T$
$\boldsymbol{r}_i$ = position vector from origin of body-fixed coordinate system to point of application of $\boldsymbol{F}_i$
T_r = rotational kinetic energy
$\boldsymbol{Y}$ = output vector obtained after N measurements, $[y_1, \ldots, y_N]^T$
$\varepsilon(\theta)$ = relative parameter error, $(\|\theta - \hat{\theta}_{\mathrm{LS}}\| / \|\theta\|) \times 100\%$
$\boldsymbol{\theta}$ = parameter vector
$\hat{\boldsymbol{\theta}}_{\mathrm{LS}}$ = estimation of parameter vector in least square estimation
$\boldsymbol{\rho}_i$ = position vector from center of mass to point of application of $\boldsymbol{F}_i$
$\sigma(\,)$ = standard deviation
υ = normalized angular rate vector
Φ = regressor matrix obtained after N measurements, $[\chi_1, \ldots, \chi_N]^T$
$\boldsymbol{\omega}$ = angular rate vector in body-fixed coordinate system, $[\omega_x \;\; \omega_y \;\; \omega_z]^T$
$\times$ = vector product
$(\cdot)|_t$ = evaluated at time t
$\|\cdot\|$ = norm of vector

Superscript

T = transpose operator

Introduction

THE increasing complexity of space vehicles, such as the Space Shuttle and space station, and their missions leads to configuration and mass property changes. Some examples of scenarios causing such changes are docking with other spacecraft, construction of a space station, launch and retrieval of satellites, an extravehicular activity (EVA) astronaut maneuvering while manipulating massive equipment components, and fuel consumption. Among these scenarios, the EVA maneuvering case is used to demonstrate application of the method proposed.

It is highly desirable, and in some cases necessary, for the attitude control system to adapt to these mass property variations without significant transformations of the control law. To achieve this, the control system must either identify the necessary mass property information, or use available measurements directly for adaptation. Both of these approaches have advantages and disadvantages but nevertheless can achieve successful control in the presence of variable or uncertain mass distribution.

The first approach, indirect adaptive control, involves two basic stages: mass property estimation and adaptation to the mass property values obtained. The accuracy of estimation is highly important because the control to be applied is based on these estimated values. Thus, available measurements should be fully utilized even during coasting maneuvers. This may be a problem for conventional estimation techniques due to the sufficient excitation condition, which states that external forces must be applied in order to drive the estimation method.[1,2] Considering that a significant part of spacecraft maneuvers is usually made up of coasting flight, it is necessary to modify the estimation method so as to use measurements during these periods as well. Sensor noise filtering is another important issue, and it makes the use of numerical differentiation undesirable. The estimation method derived and tested here solves these problems. This method is tested on models of the simplified aid for EVA rescue (SAFER),[3] which is a propulsive system developed by NASA Johnson Space Center and capable of performing various translational and attitude maneuvers. Designed as a crew member backpack, SAFER must cope with mass property variations due to changes in the size and posture of the crew member.

Equations of Motion and Estimation

The equations of motion used to describe the body dynamics depend on how accurately the actual dynamics needs to be represented. For example, the equations may include nonlinear terms representing the effect of rotating body-fixed coordinate system. They can also include various numbers of flexible modes. An equation describing the dynamics of a rigid body with uncertain mass properties is used to develop the estimation method.[4] This rotational equation of motion is written in the form

$$I\dot{\boldsymbol{\omega}} + \boldsymbol{\omega} \times I\boldsymbol{\omega} = \boldsymbol{M} + \sum_i \boldsymbol{\rho}_i \times \boldsymbol{F}_i \tag{1}$$

Mass property estimation, however, requires a different form in which the elements of the inertia matrix and coordinates of the center of mass form a vector of estimated parameters. Applied forces and torques as well as measured angular rates and/or accelerations

Received Aug. 2, 1996; revision received April 4, 1997; accepted for publication April 16, 1997.

*Ph.D. Candidate, Department of Aerospace Engineering and Engineering Mechanics.

†Associate Professor, Department of Aerospace Engineering and Engineering Mechanics. Senior Member AIAA.

are combined into a regressor matrix and output vector. This generic form

$$\Phi\boldsymbol{\theta} = \boldsymbol{Y} \tag{2}$$

is called the regression model.[5] The row vector χ_k^T is placed in the kth row of the regressor matrix Φ, whereas y_k denotes the kth element of the output vector $\boldsymbol{Y}$. They are constructed from data obtained during the kth measurement. Note that Eq. (2) is valid only if the full dynamics, including disturbances and noise, are taken into account. Otherwise, modeling errors are introduced, which affect estimation. Of course, such errors are unavoidable in practice.

Consider standard batch least square estimation (LSE) to illustrate use of the regression model [Eq. (2)] and to determine the conditions that must be satisfied for successful estimation. The LSE finds the value of the parameter vector $\hat{\boldsymbol{\theta}}_{\mathrm{LS}}$ that minimizes the quadratic cost function J of the output residuals based on all measurements available up to the current time,

$$J = \sum_k \left(y_k - \chi_k^T \hat{\boldsymbol{\theta}}_{\mathrm{LS}}\right)^2 \tag{3a}$$

$$\hat{\boldsymbol{\theta}}_{\mathrm{LS}} = (R^T R)^{-1} \Phi^T \boldsymbol{Y} \tag{3b}$$

There is no guarantee that the estimated value $\hat{\boldsymbol{\theta}}_{\mathrm{LS}}$ will be equal or even close to the actual parameter vector $\boldsymbol{\theta}$, but clearly two conditions must be satisfied to find this value. First, the output vector must be nonzero and, second, the regressor matrix must have a full rank. The latter is known as the persistency of excitation condition.[1,2,5]

Various ways to convert Eq. (1) into the regressor form have been suggested.[6–9] Some rely on linearized equations of motion; others use nonlinear combinations of parameters rather than parameters themselves. In particular, use of elements of the inverse of the inertia matrix or their products with coordinates of the center of mass may simplify conversion of Eq. (1) into the regressor model.[6,7] On the other hand, after estimating some nonlinear combinations of actual mass properties, additional computations are necessary to extract the inertia matrix and coordinates of the center of mass for later use in the control law. This increases the computation time, which is especially undesirable for an onboard recursive estimation. The method introduced utilizes complete nonlinear dynamics of a spinning rigid body to construct the regressor model. This model is, however, linear in mass properties.

Estimation Method

Estimation of the inertia matrix can be particularly intricate due to the nonlinear vector product in Eq. (1). To alleviate this problem, specific projections of the equation of motion can be found. One of them is defined by the dot product of the angular rate vector with Eq. (1),

$$\boldsymbol{\omega}^T(I\dot{\boldsymbol{\omega}} + \boldsymbol{\omega} \times I\boldsymbol{\omega}) = \boldsymbol{\omega}^T\left(\boldsymbol{M} + \sum_i \boldsymbol{\rho}_i \times \boldsymbol{F}_i\right) \tag{4}$$

This transformation eliminates the nonlinear vector product. The other term involving the inertia matrix represents time rate of change of a rotational kinetic energy T_r,

$$\dot{T}_r = \frac{\mathrm{d}}{\mathrm{d}t}\left(\frac{1}{2}\boldsymbol{\omega}^T I\boldsymbol{\omega}\right) = \frac{1}{2}\dot{\boldsymbol{\omega}}^T I\boldsymbol{\omega} + \frac{1}{2}\boldsymbol{\omega}^T I\dot{\boldsymbol{\omega}} = \boldsymbol{\omega}^T I\dot{\boldsymbol{\omega}} \tag{5}$$

which leads to a clear physical interpretation of the suggested integration

$$\int_{t_0}^{t} (\boldsymbol{\omega}^T I\dot{\boldsymbol{\omega}})\,\mathrm{d}\upsilon = \frac{1}{2}\boldsymbol{\omega}^T I\boldsymbol{\omega}\Big|_t - T_{r0} \tag{6}$$

where $T_{r0} = T_r(t_0)$.

The next step is to form the vector $\hat{\boldsymbol{I}}$ of moments and products of inertia by extracting the elements of the inertia matrix from the preceding vector-matrix product:

$$\tfrac{1}{2}\boldsymbol{\omega}^T I\boldsymbol{\omega}\Big|_t = \tfrac{1}{2}\Omega_I^T(t)\hat{\boldsymbol{I}} \tag{7}$$

where

$$\Omega_I^T(t) = \begin{bmatrix}\omega_x^2 & \omega_y^2 & \omega_z^2 & 2\omega_x\omega_y & 2\omega_x\omega_z & 2\omega_y\omega_z\end{bmatrix}\Big|_t \tag{8}$$

Finally, combining the results of Eqs. (4–7) yields

$$\frac{1}{2}\Omega_I^T(t)\hat{\boldsymbol{I}} = \int_{t_0}^{t} \boldsymbol{\omega}^T\left(\boldsymbol{M} + \sum_i \boldsymbol{\rho}_i \times \boldsymbol{F}_i\right)\mathrm{d}\upsilon + T_{r0} \tag{9}$$

The last expression is suitable for estimation of the inertia matrix if either the position of the center of mass is known or the forces applied do not produce moments relative to the center of mass. In this case, defining

$$\chi_k^T = \tfrac{1}{2}\Omega_I^T(t) \tag{10a}$$

$$y_k = \int_{t_0}^{t} \boldsymbol{\omega}^T\left(\boldsymbol{M} + \sum_i \boldsymbol{\rho}_i \times \boldsymbol{F}_i\right)\mathrm{d}\upsilon + T_{r0} \tag{10b}$$

$$\boldsymbol{\theta} = \hat{\boldsymbol{I}} \tag{10c}$$

allows construction of the regressor model [Eq. (2)]. Note that the kth measurement after t_0 is taken at time t in Eqs. (10a) and (10b).

There is one important observation about Eq. (10b): even if no forces or torques are applied, having nonzero rotational kinetic energy T_{r0} allows implementation of the method. In this case, $y_k = T_{r0} \neq 0$ and LSE based on Eq. (3b) can still be implemented provided, of course, that the regressor matrix Φ has a full rank. Physically, this means that the only condition for having a nonzero output vector $\boldsymbol{Y}$ is an initial spin of the body. However, there exist certain requirements for the maneuvers that the body undergoes to avoid singularity in the regressor matrix. These maneuvers will be discussed in detail later.

Some modifications are necessary if the position vector $\boldsymbol{R}$ of the center of mass needs to be estimated as well. Coordinates of the center of mass in the body-fixed coordinate system can be introduced into Eq. (9) by using the geometrical relationship $\boldsymbol{\rho}_i = \boldsymbol{r}_i - \boldsymbol{R}$:

$$\frac{1}{2}\Omega_I^T(t)\hat{\boldsymbol{I}} + \int_{t_0}^{t} \boldsymbol{\omega}^T(\boldsymbol{R} \times \bar{\boldsymbol{F}})\,\mathrm{d}\upsilon = \int_{t_0}^{t} \boldsymbol{\omega}^T\left(\boldsymbol{M} + \sum_i \boldsymbol{r}_i \times \boldsymbol{F}_i\right)\mathrm{d}\upsilon + T_{r0} \tag{11}$$

The scalar triple product involving $\boldsymbol{R}$ can now be transformed:

$$\boldsymbol{\omega}^T(\boldsymbol{R} \times \bar{\boldsymbol{F}}) = (\bar{\boldsymbol{F}} \times \boldsymbol{\omega})^T\boldsymbol{R} \tag{12}$$

and $\boldsymbol{R}$ be removed from the integral sign in Eq. (11) by assuming that it is constant:

$$\frac{1}{2}\Omega_I^T(t)\hat{\boldsymbol{I}} + \Omega_F^T(t, t_0)\boldsymbol{R} = \int_{t_0}^{t} \boldsymbol{\omega}^T\left(\boldsymbol{M} + \sum_i \boldsymbol{r}_i \times \boldsymbol{F}_i\right)\mathrm{d}\upsilon + T_{r0} \tag{13}$$

where

$$\Omega_F^T(t, t_0) = \int_{t_0}^{t} (\bar{\boldsymbol{F}} \times \boldsymbol{\omega})^T\,\mathrm{d}\upsilon \tag{14}$$

Equation (13) is now suitable for simultaneous estimation of both the inertia matrix and coordinates of the center of mass. Indeed, similar to Eq. (10), defining

$$\chi_k^T = \begin{bmatrix}\tfrac{1}{2}\Omega_I^T(t) & \Omega_F^T(t, t_0)\end{bmatrix} \tag{15a}$$

$$y_k = \int_{t_0}^{t} \boldsymbol{\omega}^T\left(\boldsymbol{M} + \sum_i \boldsymbol{r}_i \times \boldsymbol{F}_i\right)\mathrm{d}\upsilon + T_{r0} \tag{15b}$$

$$\boldsymbol{\theta} = [\hat{\boldsymbol{I}}^T \quad \boldsymbol{R}^T]^T \tag{15c}$$

allows construction of the regressor model [Eq. (2)]. Note again that the kth measurement after t_0 is taken at time t in Eqs. (15a) and (15b).

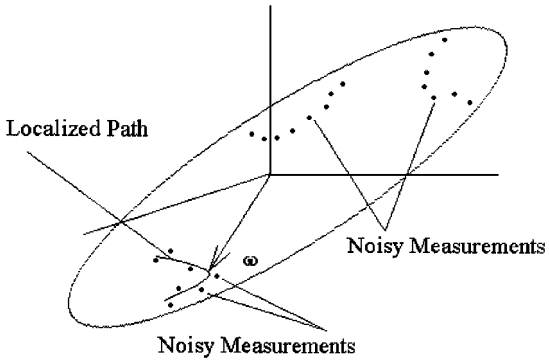

Fig. 1 Angular rate measurements with energy ellipsoid.

Estimation of Inertia Matrix and Its Geometrical Interpretation

A useful insight into mass property estimation can be obtained by looking at its geometrical interpretation. In particular, examine inertia estimation only, and to this end consider

$$\omega^T I \omega = 2T_r \tag{16}$$

which is based directly on the definition of the rotational kinetic energy. In the case of moment-free motion, the rotational kinetic energy is conserved, and hence, Eq. (16) defines an ellipsoid in the body-fixed coordinate system, called the energy (Poinsot) ellipsoid.[4] Then, the angular rate measurements in the body-fixed coordinate system should lie on the surface of this ellipsoid producing the curve, called polhode,[4] shown in Fig. 1. Moment-free motions that possess different levels of rotational kinetic energy are represented by ellipsoids of the same shape but different sizes. In particular, a higher energy level is associated with a larger ellipsoid. Applying a moment may also induce a change of rotational kinetic energy, thus, causing the ellipsoid to expand or contract without a change of shape. Nevertheless, a common geometrical representation can still be obtained if the angular rate vector in Eq. (16) is normalized by the rotational kinetic energy,

$$\upsilon^T I \upsilon = 1 \tag{17}$$

where $\upsilon = \omega / \sqrt{(2T_r)}$. All motions appear now on the same normalized energy ellipsoid defined by Eq. (17).

The estimation problem can now be looked on as a determination of magnitudes and orientations of all three axes of the normalized energy ellipsoid relative to the body-fixed coordinate system. Note that each moment-free phase still defines a polhode but it is now scaled so as to appear on the surface of the normalized ellipsoid. Also, a path on the surface of this ellipsoid may depart from the polhode due to the excitation by an applied moment. Once the moment-free motion is restored, the path follows the polhode it reached at the end of the excitation phase.

In practice, reconstruction of the ellipsoid based only on the localized path (Fig. 1) is not numerically reliable: many completely different ellipsoids can fit almost perfectly in the small region covered by a localized polhode. In fact, it can be shown that singularity occurs in the regressor matrix when the body undergoes moment-free motion or single-axis rotation. In particular, the rank deficiency of the regressor matrix is equal to one for a moment-free but not a single-axis rotation, whereas rank deficiency is equal to five for a single-axis spin regardless of a moment applied.[8] These results indicate that single-axis spin should be avoided during mass property estimation maneuvers. Also, use of several coasting maneuvers that do not lie on the same normalized polhode is suggested to prevent singularity in the regressor matrix. Alternatively, if at least one constraint for elements of the inertia matrix is known a priori, equations can be solved so that the number of columns of the regressor matrix is reduced accordingly. This makes the regressor matrix nonsingular even in the case of a single coasting maneuver excluding a pure principal axis spin.

In general, estimation can be improved by using maneuvers that cover a larger portion of the ellipsoid surface. This and some other recommendations concerning estimation of the inertia matrix are summarized as 1) use several coasting maneuvers that produce polhodes covering different areas of the ellipsoid (Fig. 1); 2) alternatively, apply moments to switch from one polhode to another in order to cover larger areas (Fig. 1); and 3) use generic dynamical properties, such as significant deviations of the angular rate vector from vicinities of the intermediate principal axis and separatrices, to cover larger areas of the ellipsoid. This, of course, requires a priori knowledge of the approximate body-fixed orientation of the principal coordinate system and separatrices, as well as their sensitivity to the uncertainties in the inertia matrix.[10,11] Thus, this approach may be suggested for fine tuning of the initial estimates of the inertia matrix.

Estimation of Center of Mass and Selection of Coordinate System

More problems arise if position of the center of mass needs to be estimated as well. In this case, the regressor matrix is clearly singular if the resultant force vector $\bar{F}$ vanishes throughout the estimation. Also, the regressor matrix is singular if the resultant force vector $\bar{F}$ remains aligned along the angular rate vector ω, however unlikely this is to happen. None of the coordinates of the center of mass can be estimated in either case. Note that conditions described so far are independent from particular choice of the body-fixed coordinate system. Selection of this coordinate system, however, is also very important because some or even all coordinates of the center of mass may become unidentifiable in such a system. For example, if the resultant force vector $\bar{F}$ remains aligned along a body-fixed axis, the corresponding body-fixed coordinate of the center of mass cannot be estimated. What is more, it is possible to have a nonzero moment applied relative to the center of mass and yet have a zero moment applied relative to the origin of the body-fixed coordinate system,

$$\sum_i \boldsymbol{r}_i \times \boldsymbol{F}_i = \boldsymbol{0}$$

Then a paradox occurs if the body, initially at rest, is spun by such a nonzero applied moment. Because the moment applied relative to the origin of the body-fixed coordinate system is zero, the output vector $\boldsymbol{Y}$ remains zero and estimation is completely impossible. One of the simplest examples of this situation is when the center of mass is offset from the line of action of a single applied force but the origin of the body-fixed coordinate system is located on this line. In general, such a choice of the origin of the body-fixed coordinate system ensures that elements put in the output vector $\boldsymbol{Y}$ during the maneuver are the same as the one at the beginning. This can also be advantageous if this initial element is nonzero. Then, standard deviations (SDs) of the elements in $\boldsymbol{Y}$ do not increase with time in the presence of sensor noise. This will be discussed in the next section.

Stochastic Analysis and Performance Evaluation

Sensor noise, unavoidable in practice, is another issue that needs to be addressed in mass property estimation. In the presence of noise, the regressor matrix constructed from angular rate measurements always has full rank. However, the regressor matrix for the true angular rate can be rank deficient. Noise, while providing excitation to sensor outputs and the regressor matrix, prevents convergence to a true optimal solution. Thus, maneuvers that produce singular regressor matrices in the absence of noise remain also unacceptable in the presence of noise.

It is clearly desirable to have an unbiased and consistent estimation.[5] The stochastic analysis, however, becomes rather complicated for this nonlinear regression problem because the noisy measurements are included not only in the output vector $\boldsymbol{Y}$ but also in the regressor matrix Φ itself. Nevertheless, certain conclusions can be drawn if the following assumptions are made: the sensor noise is white, unbiased, and Gaussian, and the noise produced by one sensor is independent from that of another sensor. In this case, it can be shown that the estimation is, in fact, biased; however, the bias is bounded, and approximately inverse proportional to the average of the squared magnitude of the angular rate vector. This result is true provided, of course, that the regressor matrix is maintained well conditioned and measurements obtained are greater than their

SDs. Also, SDs of elements of the output vector $\boldsymbol{Y}$ are assumed small. They, however, increase approximately linearly with time at a rate proportional to the moment applied relative to the origin of the body-fixed coordinate system.[8] Thus, it is generally undesirable to use prolonged excitation. The maneuvers induced by moments that are nonzero about the center of mass but are equal to zero about the origin of the body-fixed coordinate system can still be used as suggested in the preceding section. They allow the achievement of high angular rates and introduction of the required excitation while keeping SDs of the elements in $\boldsymbol{Y}$ small.

Another important practical question is validation of the estimates obtained. Although it can be shown that LES estimation is consistent under the earlier assumptions,[8] the criteria used to demonstrate this are generally too conservative to be acceptable for numerical evaluation. To this end, SDs of estimated parameters can be used; however, caution must be exercised to avoid using results based on an ill-conditioned regressor matrix. It is suggested that only the final portion of data is used for this purpose, when the condition number of the regressor matrix settles near its minimum and SDs remain relatively unchanged.

Maneuvers for Mass Property Estimation

The maneuver sequence that provides the most reliable estimation results depends on whether only estimation of the inertia matrix is necessary or estimation of the center of mass is desired as well. Clearly, the former can be accomplished if the position of the center of mass is known. Otherwise, either coasting maneuvers need to be used or excitation must be provided by force systems with zero resultant force, such as torques.

Maneuvers for Estimation of Inertia Matrix Only

Initial Spin-Up Maneuver

A torque is applied. This maneuver initiates rotation and, although it may or may not be used for mass property estimation, measurements taken are used to determine elements of the output vector $\boldsymbol{Y}$ in the subsequent maneuvers.

Supplementary Spin-Up Maneuver

Once again a torque is applied to keep the regressor matrix well conditioned. This maneuver is used for transition between coasting maneuvers. This allows for uninterrupted estimation during the sequence of excitation and coasting maneuvers. Measurements taken can be used for estimation in conjunction with data from coasting maneuvers. The disadvantage of this approach is that SDs of elements in the output vector increase during the excitation. Thus alternatively, the body can be despun and then a new initial spin-up maneuver performed.

Coasting Maneuver

Excitation is stopped but measurements are still collected into the regressor matrix during coasting. The elements of the output vector $\boldsymbol{Y}$ are all equal to the value determined at the end of the previous maneuver. Both batch and recursive estimation methods can be used. In the latter case, the condition number of the regressor matrix must be monitored and, whenever it rises above the predefined margin, one of the following must be employed.

1) Supplementary spin-up maneuver described earlier is performed.

2) The regressor matrix and parameter vector are reduced so as to ensure that the reduced regressor matrix has full rank. In this case, only some of the elements in the inertia matrix or their relative values can be estimated based on a single coasting maneuver.

3) Estimation is stopped until another coasting maneuver is performed and new data are added into regressor matrix. With a proper choice of the maneuvers this guarantees a nonsingular regressor matrix. In this case, rotation must be stopped at first and then initiated again by a new spin-up maneuver.

Maneuvers for Estimation of Inertia Matrix and Center of Mass

Initial Spin-Up Maneuver

A moment that is nonzero relative to the origin of the body-fixed coordinate system is applied. This maneuver initiates rotation and, although it may or may not be used for mass property estimation, measurements taken are used to determine elements of the output vector $\boldsymbol{Y}$ in the subsequent maneuvers.

Supplementary Spin-Up Maneuver

A moment that is zero relative to the origin of the body-fixed coordinate system is applied. This maneuver may be used for further increase of angular rates as well as for ensuring that the regressor matrix remains well conditioned. The elements of the output vector $\boldsymbol{Y}$ are all equal to the value determined at the end of the previous maneuver. Note that it may not be possible to find such a location for the origin of the body-fixed coordinate system considering that various thruster configurations can be used. In this case, location minimizing induced moments should also minimize the detrimental effect of sensor noise on the output vector. Both batch and recursive methods can be employed.

SAFER Parameter Estimation

This section describes mass property estimation of the SAFER/astronaut system (Fig. 2) (Ref. 3). From the estimation point of view, the important characteristics of this system are uncertainties in the inertia matrix and position of the center of mass due to varying masses and sizes of crew members using the maneuvering unit. Also, different positions of the crew member's legs and arms during the EVA may affect mass properties.[9] Finally, various equipment may be carried, which will not always be accounted for in the predicted mass properties. Thus, any a priori estimated values for the inertia matrix and position of the center of mass will contain errors that need to be corrected during flight testing. Another problem arises because of the low SAFER jet thrust (Table 1) and the safety considerations that restrict thrusting time. This leads to very short maneuvers and generally small angular rates in maneuvers with applied forces or torques, whereas all relatively long maneuvers are thrust free.[9] As can be seen, this situation is especially suitable for

Table 1 SAFER actuators and sensors[a]

Maneuver	M_x	M_y	M_z
Components of moment relative to center of mass, Nm			
Roll (2 thrusters)	2.9254	0	0
Pitch (2 thrusters)	0	3.0448	0
Yaw (2 thrusters)	0	0	2.2458
X (1 thruster)	0	−1.5795	1.1122
Y (1 thruster)	1.5198	0	−0.1731
Z (1 thruster)	−1.0525	0.1731	0
Components of moment relative to origin of body-fixed coordinate system, Nm			
X (1 thruster)	0	−0.0299	0.0299
Y (1 thruster)	−0.0299	0	0
Z (1 thruster)	0.0299	0	0

[a]Thrust of single thruster, 3.6 N; SD of sensor noise, 0.1 deg/s.

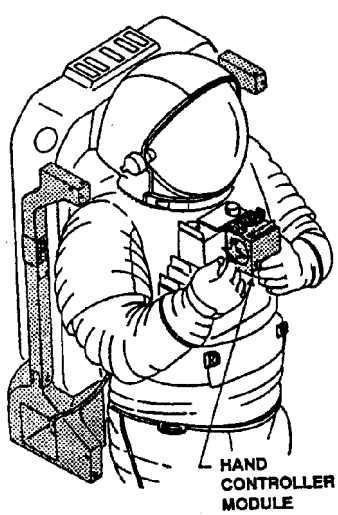

Fig. 2 SAFER general view.

using estimation methods that utilize extensive data from coasting maneuvers.

Consider results obtained from simulations of the SAFER/astronaut dynamics. Actuator and sensor characteristics of the SAFER are presented in Table 1. The thrust was determined based on linear acceleration and angular rate measurements and was verified by analysis of the propulsion system.[9] The actual mass properties are set to values given from a priori analysis. These values vary depending on the crew member's size and leg configuration, and, because the particular case is irrelevant for this analysis, the numbers shown in Table 2 are somewhat generic.[3,9]

Maneuvers simulated for estimation of the inertia matrix are shown in Figs. 3 and 4. Results of the estimation are summarized in Tables 3 and 4. They include final estimates, their SDs, and relative parameter errors. Simulations of rotational dynamics are performed in MATLAB using fourth- and fifth-order Runge–Kutta formulas. Also, trapezoidal numerical integration is utilized in the estimation method to calculate the output vector. The SDs are based on the final portion of data when their average relative changes do not exceed 1% per sample and condition number of the regressor matrix settles near its minimum (Fig. 4).

The first simulated maneuver, referred to as single spin-up, contains a 5-s spin-up due to applied positive roll torque followed by a 55-s coast (Fig. 3). Prolonged coasting is utilized for estimation of the inertia matrix. The results that are obtained both in the absence and in the presence of sensor noise are presented in Table 3 as case 1_d

Table 2 SAFER mass properties

Inertia matrix I, kgm^2				Position vector of center of mass, $\times 10^{-2}$ m		
I_x	$-I_{xy}$	$-I_{xz}$	50.07 3.5 −7.4	R_x	4.85	
$-I_{xy}$	I_y	$-I_{yz}$ = 3.5 52.66 2.1		R_y =	30.34	
$-I_{xz}$	$-I_{yz}$	I_z	−7.4 2.1 20.07	R_z	43.44	

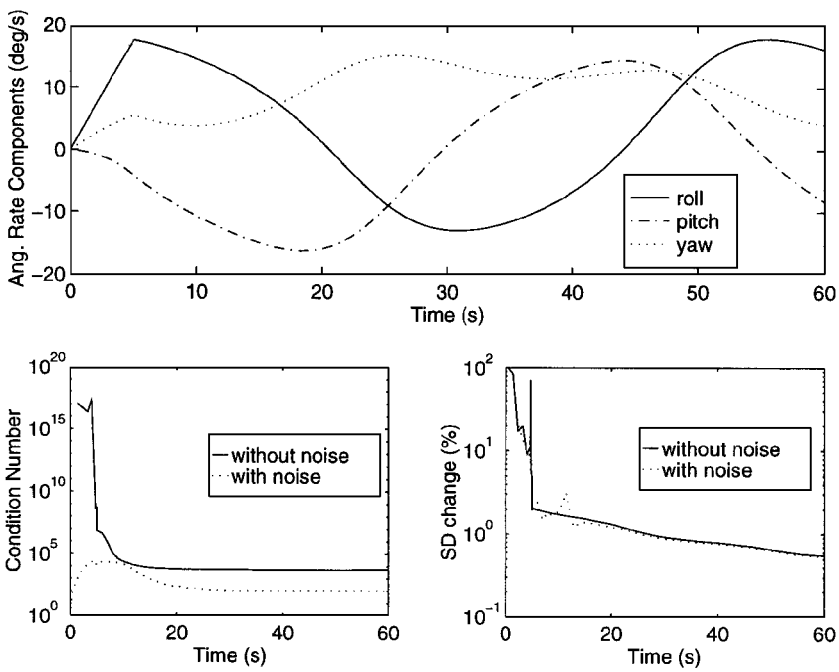

Fig. 3 Single spin-up maneuver.

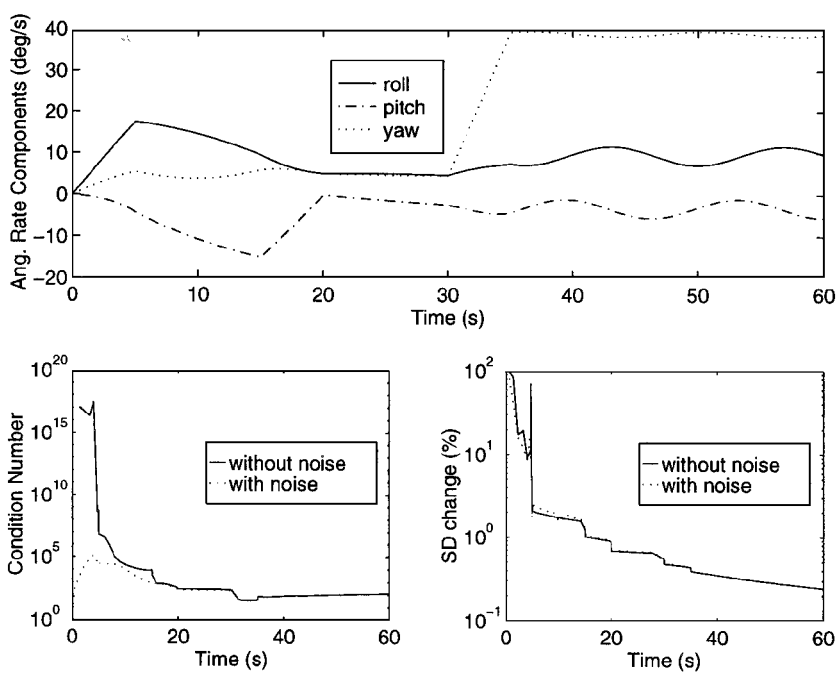

Fig. 4 Triple spin-up maneuver.

Table 3 Estimation based on single spin-up maneuver

Case no.	Estimates: Inertia matrix I, kgm^2	Estimates: SD of inertia matrix $\sigma(I)$, kgm^2	Relative parameter error $\varepsilon(I)$, %
1_d	$\begin{bmatrix} 50.1277 & 3.5577 & -7.4514 \\ 3.5577 & 52.7480 & 2.1086 \\ -7.4514 & 2.1086 & 19.9073 \end{bmatrix}$	$\begin{bmatrix} 0.0504 & 0.0404 & 0.0374 \\ 0.0404 & 0.0715 & 0.0061 \\ 0.0374 & 0.0061 & 0.1093 \end{bmatrix}$	0.3
1_n	$\begin{bmatrix} 41.8959 & -2.9634 & -1.0897 \\ -2.9634 & 41.1975 & 1.0463 \\ -1.0897 & 1.0463 & 37.7080 \end{bmatrix}$	$\begin{bmatrix} 0.8986 & 0.6728 & 0.9300 \\ 0.6728 & 1.2131 & 0.8250 \\ 0.9300 & 0.8250 & 2.3871 \end{bmatrix}$	32.1
2_d	$\begin{bmatrix} -871.2 & -740.2 & 672.2 \\ -740.2 & -1258.2 & -114.7 \\ 672.2 & -114.7 & 2009.7 \end{bmatrix}$	$\begin{bmatrix} 545.1 & 440.0 & 402.1 \\ 440.0 & 775.5 & 69.1 \\ 402.1 & 69.1 & 1177.2 \end{bmatrix}$	3623.2
2_n	$\begin{bmatrix} 42.8428 & -2.1590 & -1.8259 \\ -2.1590 & 42.5996 & 1.1712 \\ -1.8259 & 1.1712 & 35.590 \end{bmatrix}$	$\begin{bmatrix} 0.9951 & 0.8160 & 0.7441 \\ 0.8160 & 1.4309 & 0.1296 \\ 0.7441 & 0.1296 & 2.1624 \end{bmatrix}$	28.2
3_d	$\begin{bmatrix} 50.0601 & 3.5029 & -7.4014 \\ 3.5029 & 52.6515 & 2.1000 \\ -7.4014 & 2.1000 & 20.0536 \end{bmatrix}$	$\begin{bmatrix} 0.3 & 0.2 & 0.4 \\ 0.2 & 0.5 & 0 \\ 0.4 & 0 & 0.8 \end{bmatrix} \times 10^{-4}$	0.3
3_n	$\begin{bmatrix} 50.0853 & 3.6748 & -7.1784 \\ 3.6748 & 52.7930 & 2.1000 \\ -7.1784 & 2.1000 & 20.0536 \end{bmatrix}$	$\begin{bmatrix} 0.0664 & 0.0416 & 0.0751 \\ 0.0416 & 0.0998 & 0 \\ 0.0751 & 0 & 0.1784 \end{bmatrix}$	0.4

Table 4 Estimation based on triple spin-up maneuver

Case no.	Estimates: Inertia matrix I, kgm^2	Estimates: SD of inertia matrix $\sigma(I)$, kgm^2	Relative parameter error $\varepsilon(I)$, %
4_d	$\begin{bmatrix} 50.0514 & 3.4969 & -7.3927 \\ 3.4969 & 52.6390 & 2.0972 \\ -7.3927 & 2.0972 & 20.0700 \end{bmatrix}$	$\begin{bmatrix} 0.0302 & 0.0155 & 0.0442 \\ 0.0155 & 0.0150 & 0.0258 \\ 0.0442 & 0.0258 & 0.0154 \end{bmatrix}$	0.04
4_n	$\begin{bmatrix} 49.9828 & 2.9986 & -7.4819 \\ 2.9986 & 52.6778 & 2.2674 \\ -7.4819 & 2.2674 & 20.0639 \end{bmatrix}$	$\begin{bmatrix} 0.5414 & 0.3252 & 0.6978 \\ 0.3252 & 0.5219 & 0.2001 \\ 0.6978 & 0.2001 & 0.3053 \end{bmatrix}$	0.7
5_d	$\begin{bmatrix} 50.0523 & 3.4941 & -7.3942 \\ 3.4941 & 52.6360 & 2.0986 \\ -7.3942 & 2.0986 & 20.0708 \end{bmatrix}$	$\begin{bmatrix} 0.0302 & 0.0167 & 0.0393 \\ 0.0167 & 0.0279 & 0.0086 \\ 0.0393 & 0.0086 & 0.0331 \end{bmatrix}$	0.04
5_n	$\begin{bmatrix} 50.1646 & 3.1983 & -7.5188 \\ 3.1983 & 52.7741 & 2.1496 \\ -7.5188 & 2.1496 & 20.0628 \end{bmatrix}$	$\begin{bmatrix} 0.6173 & 0.3506 & 0.8051 \\ 0.3506 & 0.6018 & 0.3288 \\ 0.8051 & 0.3288 & 0.2808 \end{bmatrix}$	0.5
6_d	$\begin{bmatrix} 49.9824 & 3.4455 & -7.3013 \\ 3.4455 & 52.6234 & 2.1759 \\ -7.3013 & 2.1759 & 20.0530 \end{bmatrix}$	$\begin{bmatrix} 0.0104 & 0.0078 & 0.0184 \\ 0.0078 & 0.0114 & 0.0160 \\ 0.0184 & 0.0160 & 0.0236 \end{bmatrix}$	0.2
6_n	$\begin{bmatrix} 51.0899 & 4.0632 & -8.7031 \\ 4.0632 & 54.0876 & 2.0353 \\ -8.7031 & 2.0353 & 20.4520 \end{bmatrix}$	$\begin{bmatrix} 0.4861 & 0.9292 & 0.3281 \\ 0.9292 & 0.5208 & 0.8031 \\ 0.3281 & 0.8031 & 0.2195 \end{bmatrix}$	3.0

(deterministic) and case 1_n (noise), respectively. Also, the condition numbers of the regressor matrix and changes of SDs of the parameters are shown in Fig. 3. Estimates obtained in the absence of noise are very close to the actual values with deviations only due to numerical errors in operating with an ill-conditioned regressor matrix. When sensor noise is added, estimates become significantly biased and their deviations become larger. Such an effect is caused by a relatively low excitation during this maneuver, which is illustrated by a large condition number in the absence of noise (Fig. 3). Using the geometrical interpretation, this means that the angular rate components (Fig. 3) do not change enough to cover a significant portion of the energy ellipsoid (Fig. 1). In this case, introduction of sensor noise provides additional excitation comparable to that of the angular rate itself, which can be seen by the fact that the condition number in the presence of noise settles at a lower value (Fig. 3).

This particularly affects estimation bias because estimation of the energy ellipsoid becomes very sensitive to even small changes of the localized path. The effect of noise becomes even more apparent if only the coasting part of this maneuver is used for estimation. In the absence of noise, the singular values of the regressor matrix {0.32 0.30 0.26 0.23 0.16 0} demonstrate that its rank deficiency is equal to one. Thus, estimation of the complete inertia matrix is impossible. The only residual excitation comes from the numerical errors and produces absolutely unreliable estimates, as shown in case 2_d (Table 3). However, adding sensor noise provides enough excitation to make the regressor matrix full rank. Although the estimates, shown in case 2_n (Table 3), appear now to be closer to the actual values, they are not based on the rotational dynamics. Note that, in the absence of noise, discarding data from the initial spin-up causes an increase of the condition number by a factor of more than 10,000, from 6000 to 88×10^6, whereas, in the presence of noise, the condition number remains essentially the same: 112.04 with and 112.16 without the data from the initial spin-up. This is another indication that excitation during this maneuver is mostly due to the sensor noise.

One possible way to utilize the coasting maneuver is to reduce both the regressor matrix and parameter vector by using the a priori known value of one of the elements in the inertia matrix. The product of inertia $I_{yz} = -2.1\ \text{kgm}^2$ is assumed known, and the rest of the parameters are estimated both in the absence of noise, case 3_d, and in the presence of noise, case 3_n (Table 3). The results are dramatically improved and condition numbers are reduced from 88×10^6 to 25.75 in the absence of noise and from 112.16 to 26.05 in the presence of noise. Note that the sensor noise does not provide significant excitation in this case because the condition numbers in the absence and in the presence of noise are essentially the same.

The second simulated maneuver, referred to as triple spin-up, consists of 5-s spin-ups followed by 10-s coasting maneuvers. The spin-ups are consecutively induced by positive torques about each body-fixed axis, roll, pitch, and yaw. The maneuver is concluded by coasting, which makes its total duration equal to 60 s (Fig. 4).

As expected, greater changes of angular rate components occur during this maneuver. Consequently, a larger portion of the energy ellipsoid is covered and better estimates are obtained in the absence of noise (case 4_d) and in the presence of noise (case 4_n), as shown in Table 4. Another evidence of greater excitation is provided by the condition numbers of the regressor matrix (Fig. 4): the condition numbers in the absence and in the presence of noise become very close as more measurements are used in the regressor matrix. Also, the condition number in the absence of noise is lower than that of the previous maneuver (Fig. 4).

The last simulated maneuver, referred to as thrusting, includes an initial 2-s spin-up by a positive roll torque, which is followed by three consecutive excitations. Each excitation is induced by a 10-s firing of a single thruster in the positive x, y, and z directions, respectively. After that, a negative roll torque is applied for 2 s, which is similarly followed by 10-s firings in the negative x, y,

Table 5 Simultaneous estimation of inertia and center of mass

Case no.	Estimates: Inertia matrix I, kgm^2	SD of inertia matrix $\sigma(I)$, kgm^2	Relative parameter error $\varepsilon(I)$, %	Position vector of center of mass $\boldsymbol{R}$, $\times 10^{-2}$ m	SD of center of mass $\sigma(\boldsymbol{R})$, $\times 10^{-2}$ m	Relative parameter error $\varepsilon(\boldsymbol{R})$, %
7_d	$\begin{bmatrix} 50.0186 & 3.4887 & -7.3882 \\ 3.4887 & 52.6057 & 2.0971 \\ -7.3882 & 2.0971 & 20.0684 \end{bmatrix}$	$\begin{bmatrix} 0.0218 & 0.0022 & 0.0033 \\ 0.0022 & 0.0236 & 0.0012 \\ 0.0033 & 0.0012 & 0.0109 \end{bmatrix}$	0.1	$[4.86 \quad 30.33 \quad 43.46]^T$	$[0.005 \quad 0.019 \quad 0.020]^T$	0.04
7_n	$\begin{bmatrix} 48.7586 & 3.3190 & -7.1641 \\ 3.3190 & 51.2635 & 2.0708 \\ -7.1641 & 2.0708 & 19.7416 \end{bmatrix}$	$\begin{bmatrix} 0.6309 & 0.0843 & 0.1070 \\ 0.0843 & 0.6616 & 0.1833 \\ 0.1070 & 0.1833 & 0.3388 \end{bmatrix}$	2.6	$[4.75 \quad 29.80 \quad 42.53]^T$	$[0.40 \quad 0.90 \quad 1.82]^T$	2.0

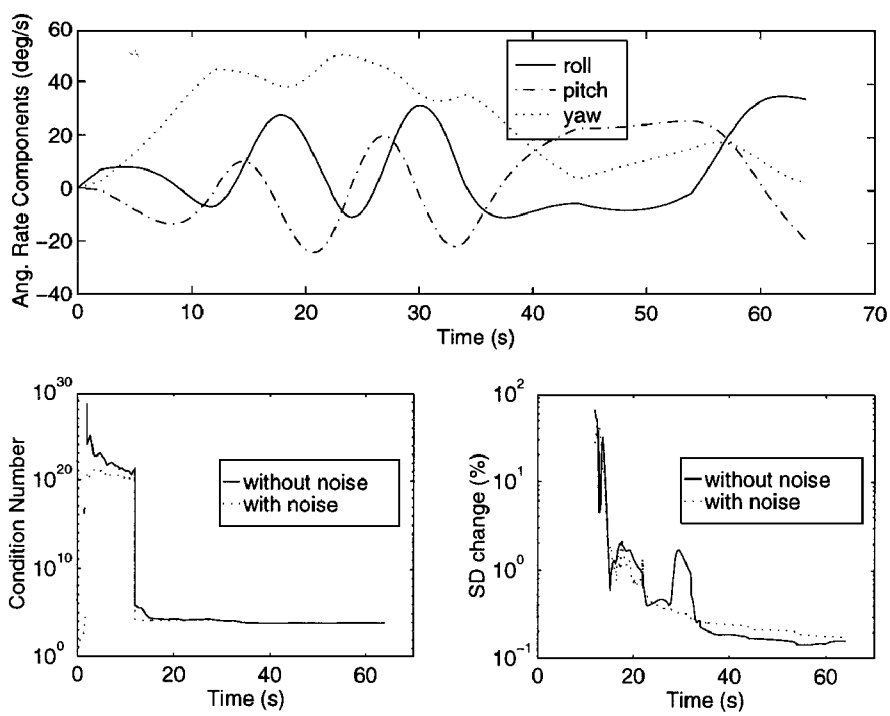

Fig. 5 Thrusting maneuver.

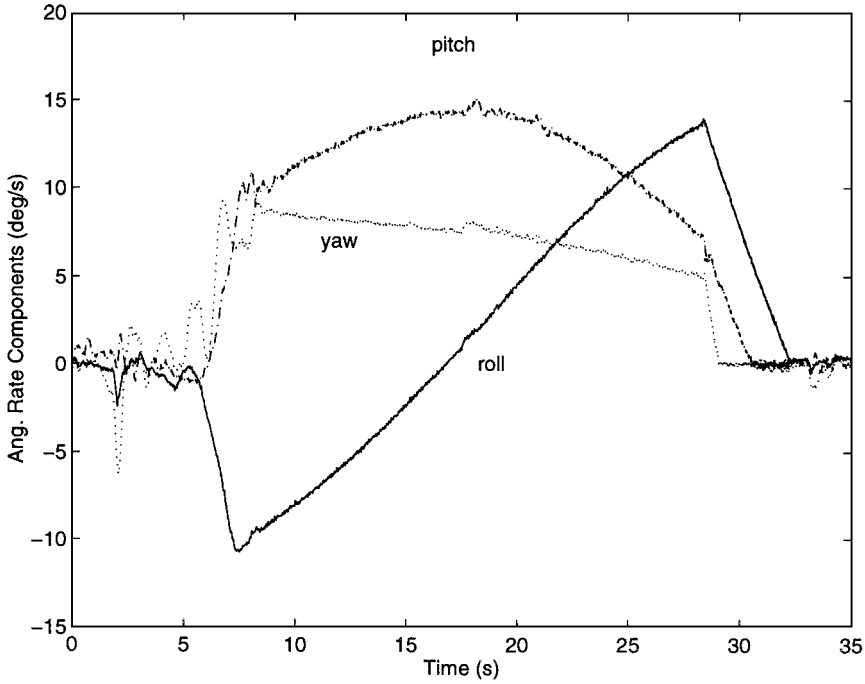

Fig. 6 Multiaxis rotation example of rate sensor data from STS-64 EVA.

Table 6 Environmental effects on SAFER (altitude, 300 km)

Environmental phenomenon	Magnitude of moment relative to center of mass, $\times 10^{-4}$ Nm
Gravity gradient	0.76
Aerodynamic drag	7.00
Solar radiation	0.05
Acceptable maneuver duration $\approx$ 60 s	

and z directions (Fig. 5). This maneuver is used for simultaneous estimation of the inertia matrix and position of the center of mass. Results are summarized in Table 5 in the absence (case 7_d) and in the presence of noise (case 7_n). They include estimates, their SDs, and relative parameter errors for both the inertia matrix and the position vector of the center of mass. Note that the lines of action of the forces produced by each firing of a single SAFER thruster do not intersect at one point. Therefore, the body-fixed coordinate system can only be placed so as to minimize the moments induced relative to its origin (Table 1).

An EVA crew member equipped with SAFER, just as any spacecraft, is subjected to various environmental forces and moments. Primary examples include gravity gradient torque, aerodynamic drag, and solar radiation pressure. Their influence must be evaluated to ensure accuracy of the estimation. These effects generally depend on the mass properties and geometry of the vehicle as well as orbital parameters. Thus, the values obtained for the SAFER/astronaut system are based on the worst-case scenario and are somewhat generic. They are summarized in Table 6. The acceptable maneuver duration is based on the time elapsed until the angular rate deviation due to environmental effects becomes comparable to the SD of the sensor noise.

This method was also used to analyze data gathered during an EVA with SAFER on the STS-64 mission in September 1994. An example of rate sensor measurements taken at a sampling rate of 50 Hz is shown in Fig. 6. The resulting estimated inertia matrix

$$I = \begin{bmatrix} 41.9973 & 1.3335 & -2.2756 \\ 1.3335 & 41.5098 & 0.2439 \\ -2.2756 & 0.2439 & 16.3168 \end{bmatrix} \text{ kgm}^2$$

illustrates the performance of the method and is based on rotational maneuvers performed by astronaut Mark Lee (crew member EV1).

Conclusions

The method described for mass property estimation allows efficient use of angular rate measurements during coasting maneuvers. The elements of the inertia matrix and coordinates of the center of mass are estimated directly and, if desired, simultaneously. Estimation performed for various SAFER/astronaut maneuvers, both simulated and actual, demonstrated the usefulness of the method.

Acknowledgments

This work was supported by Grant NAG9-766 from NASA Johnson Space Center, with Technical Monitor Clifford W. Hess.

References

[1] Mareels, I. M. Y., Bitmead, R. R., Gevers, M., Johnson, C. R., Kosut, R.L., and Paubelle, M. A., "How Exciting Can a Signal Really Be?" *Systems and Control Letters*, Vol. 8, No. 3, 1987, pp. 197–204.

[2] Janecki, D., "Persistency of Excitation for Continuous-Time Systems—Time-Domain Approach," *Systems and Control Letters*, Vol. 8, No. 4, 1987, pp. 333–344.

[3] NASA, "Simplified Aid for EVA Rescue (SAFER) Training Manual," NASA Johnson Space Center, Rept. JSC-26283, Houston, TX, July 1993.

[4] Hughes, P., *Spacecraft Attitude Dynamics*, Wiley, New York, 1986, pp. 39–138.

[5] Åström, K. J., and Wittenmark, B., *Adaptive Control*, 2nd ed., Addison–Wesley, Reading, MA, 1995, pp. 41–90.

[6] Bergmann, E. V., Walker, B. K., and Levy, D. R., "Mass Property Estimation for Control of Asymmetrical Satellites," *Journal of Guidance, Control, and Dynamics*, Vol. 10, No. 5, 1987, pp. 483–491.

[7] Richfield, R. F., Walker, B. K., and Bergmann, E. V., "Input Selection for a Second-Order Mass Property Estimator," *Journal of Guidance, Control, and Dynamics*, Vol. 11, No. 3, 1988, pp. 207–212.

[8] Tanygin, S., "Parameter Estimation and Adaptive Control of Bodies with Variable Mass Distribution," M.S. Thesis, Dept. of Aerospace Engineering, Univ. of Cincinnati, Cincinnati, OH, June 1996.

[9] Williams, T., Tanygin, S., and Bolender, L., "SAFER Mass Properties Determination: Results from On-Orbit Data," *Proceedings of 1995 AAS/AIAA Astrodynamics Specialist Conference*, Advances in the Astronautical Sciences, Vol. 90, Pt. 1, Univelt, San Diego, CA, 1995, pp. 573–592.

[10] Williams, T., and Tanygin, S., "Dynamics of a Near-Symmetrical Spacecraft Driven by a Constant Thrust," *Proceedings of 6th AAS/AIAA Spaceflight Mechanics Meeting*, Advances in the Astronautical Sciences, Vol. 93, Pt. 2, Univelt, San Diego, CA, 1996, pp. 925–944.

[11] Williams, T., and Tanygin, S., "Dynamics of an Asymmetric Spacecraft Driven by a Constant Thrust: Perturbation Studies," 7th AAS/AIAA Spaceflight Mechanics Meeting, AAS Paper 97-114, Huntsville, AL, Feb. 1997.